

## Surface Wind Vergence over the Tropical Indian Ocean<sup>1</sup>

MICHAEL HANTEL<sup>2</sup>

*Meteorologisches Institut der Universität Bonn, Germany*

(Manuscript received 15 February 1971, in revised form 8 June 1971)

### ABSTRACT

From surface wind estimates published in the Dutch Atlas monthly charts of surface wind vergence over the Indian Ocean down to 50S were computed. Since the original data were smoothed by a low-pass filter, the charts exhibit only regional and large-scale features. The vergence distributions are not zonally symmetric; rather, they show a cell-like structure.

The vergence patterns are discussed in terms of latitudinal-time sections, both for the Arabian Sea and the Bay of Bengal longitude range, and compared with similar plots of the precipitation frequency. North of 10–20S there seem to exist three different circulation regimes, separated by sharply defined transition periods, a characteristic of the Indian monsoon climate. A simple description of this threefold monsoonal rhythm is given in terms of the first and second harmonics of the annual march of temperature.

### 1. Introduction

This study is a descriptive contribution toward the sea surface climatology of the Indian Ocean. Based on the 2° by 2° latitude-longitude monthly surface wind force<sup>3</sup> data of the Atlas of the Koninklijk Nederlands Meteorologisch Instituut [hereafter referred to as the "Dutch Atlas" (1952)], monthly charts of the wind vergence were compiled for the Indian Ocean down to 50S, between the northern land boundaries and longitudes 20 and 116E.

A recent effort to calculate the wind vergence from the Dutch Atlas data for a single month (van Dijk, 1956) seemed to be discouraging. Van Dijk's vergence chart for January was apparently over-detailed. The present study avoids this drawback by an objective smoothing procedure that filters out small-scale details below a certain wavelength. This method improves considerably the appearance of the vergence patterns and allows for a comparison with other climatic elements.

The surface wind vergence is intimately related to vertical motions in the atmospheric boundary layer. Applying the Boussinesq approximation, and vertically integrating the continuity equation, one obtains

$$w_H = - \int_0^H \text{div}_2 \mathbf{V} dz, \quad (1)$$

<sup>1</sup> Paper presented at the AMS-IMS International Conference on Meteorology, 30 November–4 December 1970, Israel.

<sup>2</sup> This work was carried out during a summer visit in the Advanced Study Program at the National Center for Atmospheric Research, Boulder, Colo. The National Center for Atmospheric Research is sponsored by the National Science Foundation.

<sup>3</sup> Speed estimates based on Beaufort scale.

where  $w_H$  is the vertical velocity at the level  $H$ ,  $w_0$  is assumed to be zero,  $\mathbf{V}$  is the horizontal wind vector, and  $\text{div}_2$  denotes the two-dimensional vergence operator. We prefer to use the term vergence instead of divergence and reserve divergence for positive vergence, convergence for negative vergence. Eq. (1) allows us to estimate the vertical velocity at a level  $H$  not too high ( $\leq 1000$  m) so that the surface vergence fairly represents the average vergence between 0 and  $H$ . For observed large-scale values of the order  $|\text{div}_2 \mathbf{V}_0| = 5 \times 10^{-6} \text{ sec}^{-1}$ , Eq. (1) yields vertical velocities of the order  $|w_H| = 0.1 \text{ cm sec}^{-1}$ .

For these reasons one expects some correspondence between vergence and precipitation. Riehl (1954) has noted the correlation between vergence and rainfall amount and Flohn (1957) has extended the analysis to average cloudiness and precipitation frequency. Fig. 1 is a scatter diagram of surface vergence vs precipitation frequency in the tropical Atlantic Ocean (10S–10N) according to Flohn (1957). The correlation coefficient is 0.88 for the Northern Hemisphere winter and 0.90 for northern summer. Fig. 1 is based on 366,000 single observations, every point being valid for a latitude interval of 1°. The excellent correlation of the diagram should not mislead us to conclude that precipitation in the tropics is a unique function of the vergence field, since tropical convection is not randomly distributed (Riehl, 1954). It is obvious, however, that the vergence is a valuable tool for assessing the dynamic interaction between the wind and precipitation fields, in particular their singularities in connection with the monsoonal rhythm.

Treatment of the data, the filtering procedure, and basic results are briefly outlined in the next section; a

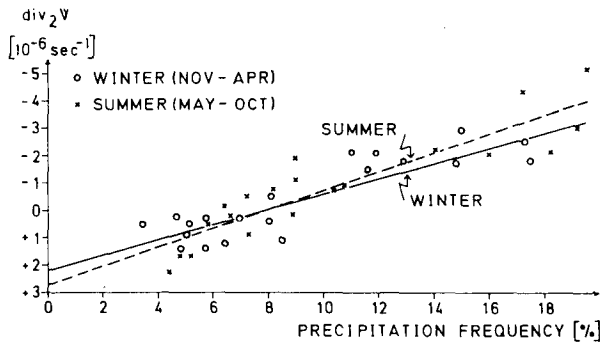


FIG. 1. Surface wind vergence ( $10^{-6} \text{ sec}^{-1}$ ) vs precipitation frequency (%). Data are valid for the Atlantic Ocean from 10S-10N (after Flohn, 1957).

more thorough discussion of these subjects, together with the complete set of the monthly charts, is given elsewhere (Hantel, 1971). In Section 3 the vergence patterns are compared with the precipitation frequency and with the annual march of tropospheric temperature. Some conclusions are drawn in the last section.

2. Data and basic results

The wind force data published in the Dutch Atlas are mainly based on meteorological logbooks of Dutch, German, British and Swedish ships. The data are presented in the Atlas as monthly climatological means of surface wind speed and direction for every  $2^\circ$  by  $2^\circ$  latitude-longitude square. It should be stressed that wind force estimates are by no means a poor substitute for modern wind speed measurements. From the work of Verploegh (1967) it is known that the accidental errors of wind measurement aboard research vessels have the same order of magnitude as those of wind estimates made by experienced observers. According to Verploegh, this order of magnitude is  $0.58 I$ , where  $I$

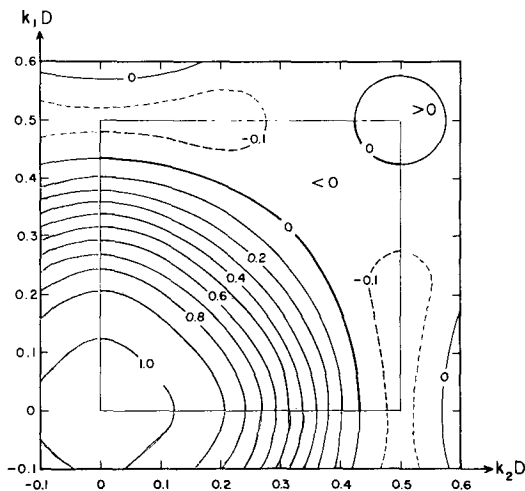


FIG. 2. Wavenumber response,  $H(k_1, k_2)$ , of filter weight function, using values inside square box only.

TABLE 1: Equivalent wind speeds ( $\text{m sec}^{-1}$ ) based on the Beaufort scale.

Beaufort values	0-0.4	1	2	3	4	5	6	7
Wind speed	0.3	1.0	2.8	4.6	6.8	9.3	12.0	14.9

denotes the Beaufort interval. This result should clearly demonstrate the value of wind force data obtained by simple observation. In particular, the wind estimates on which the Dutch Atlas data are based deserve full confidence concerning their accuracy and reliability.

The main elements of inaccuracy of the present compilation are a result of the following:

1) The uneven coverage of the data. There are some  $2^\circ$  by  $2^\circ$  latitude-longitude squares along shipping routes with as many as 2000 single observations per month, whereas other fields contain less than 5. For fields of the latter type, the Dutch Atlas does not give wind force values. In the present compilation these gaps were filled by linear interpolation from neighboring fields; they are marked by dots on the vergence charts.

2) The necessity of converting mean wind force into mean wind speed, instead of converting actual wind forces into actual wind speeds and then averaging. The difference between the two averaging techniques is due to the nonlinearity of the Beaufort scale (Table 1).

The completed patterns of the zonal  $u$  and meridional

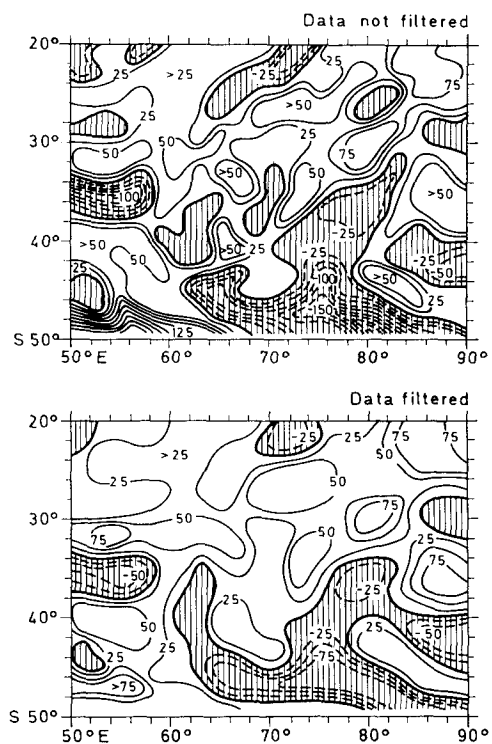


FIG. 3. Filtered and non-filtered surface wind vergence ( $10^{-6} \text{ sec}^{-1}$ ) for July. Areas of convergence are hatched. Upper part: data not filtered. Lower part: data filtered.

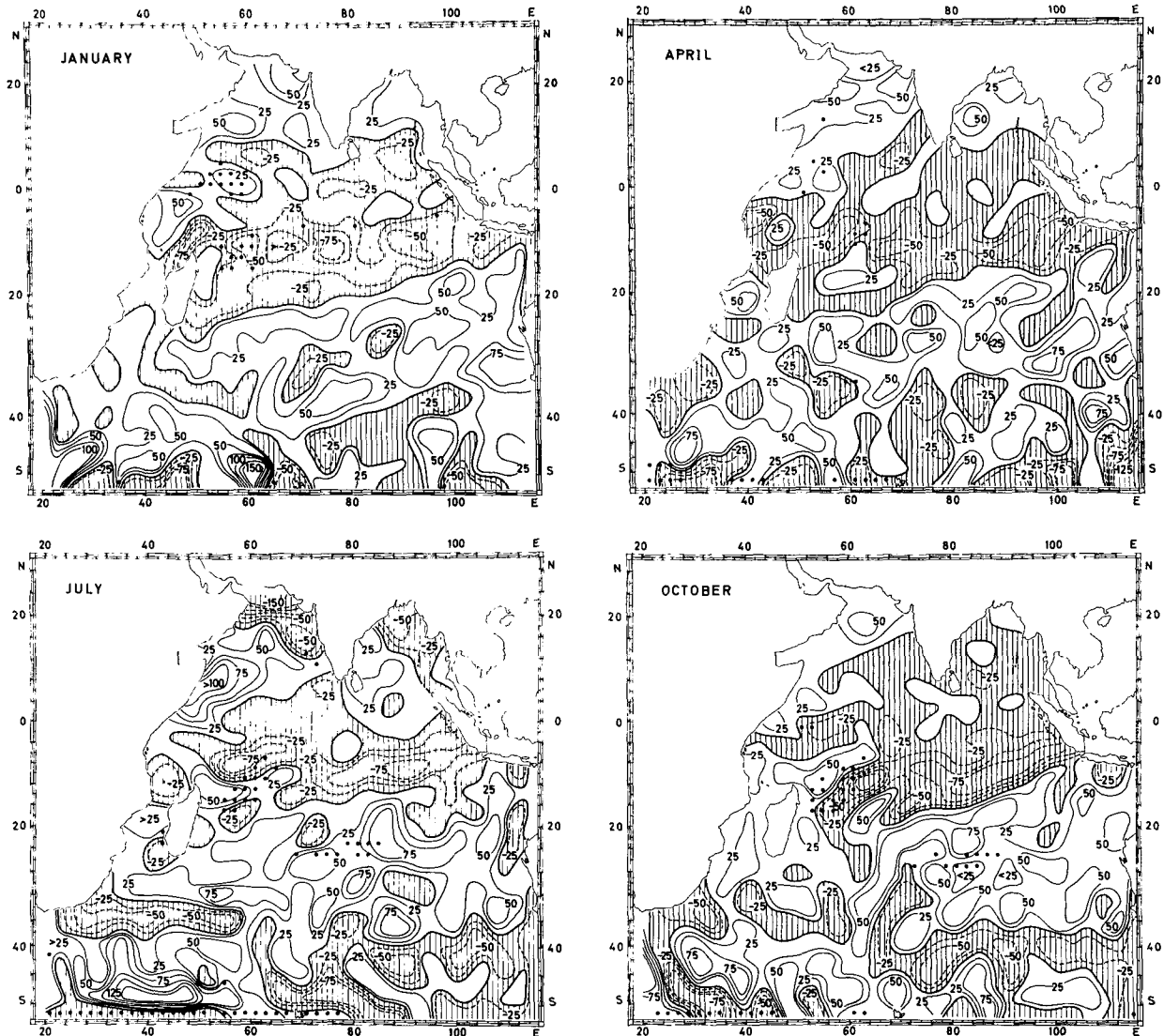


FIG. 4. Surface wind vergence ( $10^{-7} \text{ sec}^{-1}$ ) for January, April, July and October. Areas of convergence are hatched. Dots indicate  $2^\circ$  by  $2^\circ$  latitude-longitude squares without available wind data.

$v$  wind components were smoothed by an objective filtering procedure. The filter operator consists of a 5 by 5 discrete weight function (Bleck, 1965), and was applied once to each of the  $u$  and  $v$  fields. Its attenuation factor or wavenumber response function is

$$H(k_1, k_2) = \frac{A^*(k_1, k_2)}{A(k_1, k_2)}, \quad (2)$$

where  $A$  is the original amplitude of a particular spectral component pertinent to the wavenumbers  $k_1, k_2$  in the meridional and zonal direction, respectively, and  $A^*$  is the filtered amplitude of this partial wave. Since the wavenumbers  $k_1, k_2$  are measured in terms of the grid distance  $D = 2^\circ$  latitude or longitude,  $kD$  values are pure numbers. Fig. 2 shows  $H$  to have values of about

0.5 in the vicinity of  $kD \approx 0.25$  which is one-half of the Nyquist wavenumber. Therefore, the attenuation factor for climatologically significant waves with wavelengths  $> 5$  grid intervals (corresponding to  $kD \leq 0.2$ ) is fairly close to 1, whereas the factor for noise waves with wavelengths, say,  $< 3$  grid intervals (corresponding to  $kD \geq 0.33$ ) is reasonably close to zero. Hence, this smoothing function operates as a low-pass filter. It is objective in the sense that it eliminates, in a well-defined manner, the small-scale, noisy fluctuations from the data which tend to blur the significant patterns. The filter cannot, however, in any way correct for the uneven coverage, i.e., representativeness of the data. Fig. 3 shows the effectiveness of the filter procedure.

The vergence was computed by applying a simple finite-difference formulation of the two-dimensional

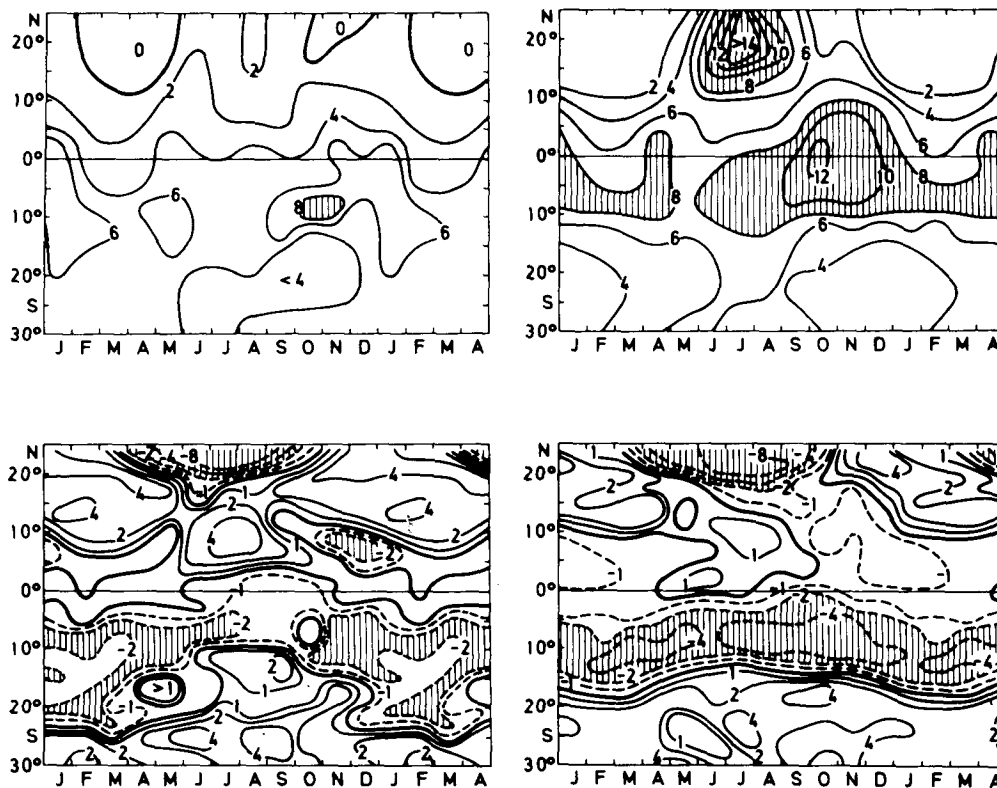


FIG. 5. Zonal averages of precipitation frequency (percent, top) and wind vergence ( $10^{-6} \text{ sec}^{-1}$ , bottom) for longitudes appropriate to the Arabian Sea (50-70E, left) and the Bay of Bengal (80-100E, right).

divergence operator on the filtered wind field (Hantel, 1971). The surface wind vergence charts for the main months of the four seasons are presented in Fig. 4. They are in general agreement with the early compilations of Mintz and Dean (1952) for January and July based on  $5^\circ$  by  $5^\circ$  square averages. Some of the more important features of Fig. 4 are as follows:

- 1) The average magnitude of the large-scale surface vergence is of the order  $(1-10) \times 10^{-6} \text{ sec}^{-1}$ .
- 2) There is a general tendency of the surface air motion over the Indian Ocean to be convergent in the inner tropics and divergent in the subtropics and over the winter monsoon area. However, this tendency does not show up in form of a zonally symmetric distribution of the vergence, but rather in form of a cell-like structure.
- 3) One of the most prominent of these cells is the divergent area around the East African Cape. As has been pointed out recently (Flohn *et al.*, 1968), this region is characterized by large-scale subsidence and minimum precipitation and is identical with the lowest position of the inversion base level. In particular, it is related to Findlater's (1970) low-level jet over the western Indian Ocean in the Northern Hemisphere summer.
- 4) The main convergent and divergent areas are in

rough agreement with the computer-produced cloud pictures prepared by Kornfield and Hasler (1969). This applies particularly to the convergent cells in the vicinity of the intertropical convergence zone (ITCZ).

### 3. Monsoonal fluctuations

The climatological significance of the monthly vergence charts can be more clearly demonstrated by means of Fig. 5 which exhibits latitudinal-time sections of precipitation frequency and vergence. The ordinate of each of the single pictures of Fig. 5 is geographical latitude, the abscissa the time of the year, running not from January until December but from January to April in order to show the northern winter as a whole. Some obvious qualitative conclusions are as follows:

- 1) For both the Arabian Sea and the Bay of Bengal region there seem to exist at least two different circulation regimes north of approximately 10-20S. The summer regime lasts from May-June until September-October. It is characterized by a pattern of wind vergence and precipitation frequency that is different from the pattern for the rest of the year. During northern summer, we observe strong convergence north of 15N with considerable precipitation values; between 15N and the equator, divergence and relative dryness

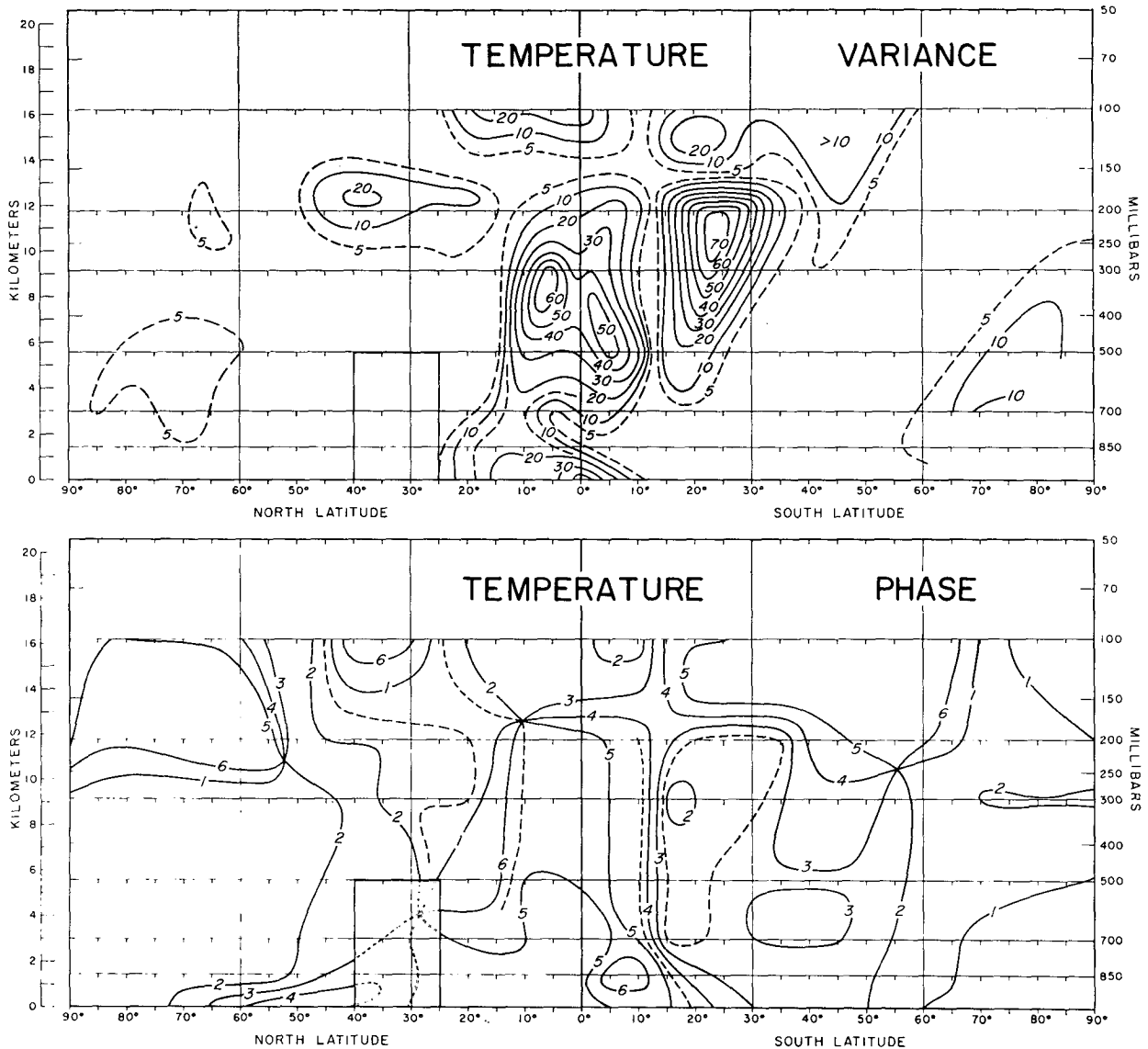


FIG. 6. Height variation of the second harmonic of temperature, zonally-averaged between 60 and 120E (according to van Loon and Jenne, 1970). The two parts depict the contribution of the second harmonic to total variance (top) and the month of the first maximum of the second harmonic (bottom).

prevails. Compared with this Indian summer monsoon distribution, the winter pattern is almost reversed.

2) If one defines the ITCZ as the zone of maximum convergence, there exists a well-developed ITCZ throughout the year in the Southern Hemisphere, its core being situated around 10S and oscillating equatorward in summer and southward in winter. This is in accordance with the precipitation frequency pattern.

3) Over the Arabian Sea there exists a secondary maximum of convergence in the Northern Hemisphere. It is located between 5–10N and lasts from September until May, interrupted during June–August by a divergent period. During November–January the convergence is comparatively strong; one might call this

period the winter ITCZ period. There is no strong support for a double ITCZ in the Bay of Bengal region in any season of the year. Therefore, the hypothesis of a well-developed double ITCZ over the entire Indian Ocean throughout the year is not supported by the present data. In addition, these observations are in fair agreement with the cloud pictures seen from satellites (Kornfeld and Hasler, 1969).

4) The transition between the winter and the summer regimes does not seem to be continuous. During the burst of the monsoon, in May–June, the Arabian Sea northern ITCZ vanishes abruptly. A similarly fast transition seems to take place in September–October, with a third (mainly seen in the precipitation frequency)

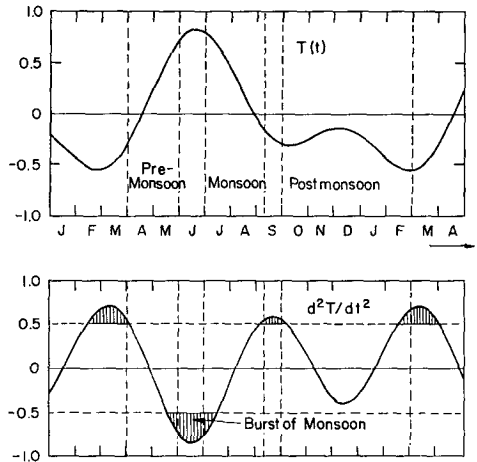


FIG. 7. Schematic pattern of possible monsoonal rhythm showing the functions  $T(t)$  [Eq. (3), top] and  $d^2T/dt^2$  [Eq. (4), bottom]. The time coordinate is in months with  $t=0-1$  (January), 1-2 (February), etc., and the ordinate is in arbitrary units.

in January-February, separating different circulation configurations. The sharp time-gradients of all quantities during the transition stages prevent one from describing the Indian circulation as a harmonic oscillation. Rather, one has to look at it as a flipflop-like oscillation between relatively steady states with discontinuous jumps from one state to the other. Jumps of this kind are characterized by sizeable contributions of higher harmonics.

The latter viewpoint is supported by recent data compilations of van Loon and Jenne (1970) which, for the annual march of temperature, indicate a strong influence of the second harmonic. Fig. 6 gives the fraction of the total variance of mean temperature that is attributed to the second harmonic, as well as the phase of the second harmonic. The data are zonal averages between 60 and 120E. A prominent feature of Fig. 6 is a cell throughout most of the troposphere between 10-15N in which the second harmonic shows significant values. This cell has a fairly uniform phase of the first maximum of the second harmonic, namely, May-June. Similar plots for the first harmonic show its phase to be between April and August, a representative month being June. Higher harmonics than the second do not significantly contribute to the total variance (H. van Loon, personal communication).

Consequently, one is tempted to describe the combined oscillation in terms of a superposition of the two first harmonics, with wavelengths of one year and one-half year, respectively, and with corresponding phases. This function is given by

$$T = 0.6 \cos \frac{2\pi}{12}(t-6.0) + 0.4 \cos \frac{4\pi}{12}(t-5.5), \quad (3)$$

where  $t$  is the time coordinate in months. Hence we

assume the contribution of the second harmonic to the total variance to be of the order of  $(0.4)^2 / [(0.6)^2 + (0.4)^2] \approx 30\%$ , in accordance with the upper part of Fig. 6. Fig. 7 shows the function  $T(t)$  together with its second derivative

$$\frac{d^2T}{dt^2} = -\left(\frac{2\pi}{12}\right)^2 \left[ 0.6 \cos \frac{2\pi}{12}(t-6.0) + 1.6 \cos \frac{4\pi}{12}(t-5.5) \right] \quad (4)$$

in arbitrary units. We consider the extreme values of the second derivative as indicators for the jump stages. The greatest value of  $d^2T/dt^2$  in May-June may be representative for the burst of the Indian monsoon. Weaker transition periods in February-March from the winter to the premonsoon stage and in September, denoting the end of the summer monsoon and the beginning of the postmonsoonal period, are also present (Trewartha, 1961). Surprisingly, these main transition states seem to match roughly the surface observations of Fig. 5, although the functions (3) and (4) are concerned only with the annual march of temperature and not precipitation.

#### 4. Conclusion

Keeping in mind that any surface climatology must be intimately related to upper air processes, the coincidence between sea surface wind vergence and tropospheric temperature patterns as discussed in the previous section confirms the characteristic mechanism of abrupt change between different circulation regimes over the Indian Ocean extending far into the Indian subcontinent. The observational fact of sharp transition stages which separate relatively steady periods indicates the existence of some kind of complex instability during such transitions, in particular during the monsoon burst.

This mechanism, however, still needs to be explained in terms of dynamical models. It might be stressed, therefore, that the speculative scheme of Fig. 7 can be considered neither as an appropriate description of the South Asiatic monsoon nor as a theoretical explanation of it. It only simulates in the simplest possible formulation the two features the author considers to be the most essential ones of the Indian monsoon climate: the threefold rhythm and the sharp transition stages (Ramage, 1971, Chap. 5). These two features are closely connected. Sharp transition stages are not possible if there are only two seasons (provided only annual and semiannual waves are present); conversely, if there are three seasons, relatively sharp transition stages must appear. Fig. 6 has shown the second harmonic of temperature to be confined to the tropical region. It is hard to believe that this is not an essential element of the monsoon which is confined to just this region (Ramage, 1971).

*Acknowledgments.* Thanks are due to Prof. H. Flohn, Director of the Meteorological Institute of the University of Bonn, and to Prof. H. van de Boogaard, National Center for Atmospheric Research, for extensive discussions and for suggesting many aspects of this study. Valuable comments of Dr. H. van Loon, National Center for Atmospheric Research, concerning the time-spectra of temperature and other variables are gratefully acknowledged, as are the constructive criticisms of the reviewers.

The numerical calculations were carried out on the IBM 7090/1410 computer of the "Gesellschaft für Mathematik und Datenverarbeitung" at the University of Bonn. The National Center for Atmospheric Research provided generous support for the final version of the manuscript.

## REFERENCES

- Bleck, R., 1965: Lineare Approximationsmethoden zur Bestimmung ein- und zweidimensionaler numerischer Filter der dynamischen Meteorologie. Tech. Rept., Institut für Theoretische Meteorologie der Freien Universität Berlin, 86 pp.
- Dutch Atlas, 1952: Indische Oceaan, Oceanografische en Meteorologische Gegevens. *Konink. Ned. Meteor. Inst.*, No. 135, 31 pp, 24 maps.
- Findlater, J., 1970: A major low-level air current near the Indian Ocean during the northern summer (article), and inter-hemispheric transport of air in the lower troposphere over the western Indian Ocean (Discussion). *Quart. J. Roy. Meteor. Soc.*, **96**, 551-554.
- Flohn, H., 1957: Studien zur Dynamik der äquatorialen Atmosphäre. I: Horizontale und vertikale Windkomponenten auf dem Atlantik. *Beitr. Phys. Atmos.*, **30**, 18-46.
- , M. Hantel and E. Ruprecht, 1968: Air-mass dynamics or subsidence processes in the Arabian Sea summer monsoon? *J. Atmos. Sci.*, **25**, 527-529.
- Hantel, M., 1971: Monthly charts of surface wind vergence over the tropical Indian Ocean. *Bonner Meteor. Abhandl.*, No. 14, 31-79.
- Kornfield, J., and A. F. Hasler, 1969: A photographic summary of the earth's cloud cover for the year 1967. *J. Appl. Meteor.*, **8**, 687-700.
- Mintz, Y., and G. Dean, 1952: The observed mean field of motion of the atmosphere. Geophysical Research Papers No. 17, Air Force Cambridge Research Center, 65 pp.
- Ramage, C. S., 1971: *Monsoon Meteorology*. New York, Academic Press, 296 pp.
- Riehl, H., 1954: *Tropical Meteorology*. New York, McGraw-Hill, 392 pp.
- Trewartha, G. T., 1961: *The Earth's Problem Climates*. The University of Washington Press, 334 pp.
- van Dijk, W., 1956: An investigation of the vergence field of the wind and ocean currents of the Indian Ocean. *Arch. Meteor., Geophys. Bioklim.*, **A9**, 158-177.
- van Loon, H., and R. L. Jenne, 1970: On the half-yearly oscillations in the tropics. *Tellus*, **22**, 391-398.
- Verploegh, G., 1967: Observation and analysis of the surface wind over the ocean. *Mededel. Verhandel.*, **89**, 67 pp.